



**HAL**  
open science

# Importance of interfacial step alignment in hetero-epitaxy and orientation relationships: the case of Ag equilibrated on Ni substrates. Part 1 computer simulations

P. Wynblatt, D. Chatain

► **To cite this version:**

P. Wynblatt, D. Chatain. Importance of interfacial step alignment in hetero-epitaxy and orientation relationships: the case of Ag equilibrated on Ni substrates. Part 1 computer simulations. *Journal of Materials Science*, 2015, 50 (15), pp.5262-5275. 10.1007/s10853-015-9074-1 . hal-01162453

**HAL Id: hal-01162453**

**<https://hal.science/hal-01162453>**

Submitted on 4 May 2018

**HAL** is a multi-disciplinary open access archive for the deposit and dissemination of scientific research documents, whether they are published or not. The documents may come from teaching and research institutions in France or abroad, or from public or private research centers.

L'archive ouverte pluridisciplinaire **HAL**, est destinée au dépôt et à la diffusion de documents scientifiques de niveau recherche, publiés ou non, émanant des établissements d'enseignement et de recherche français ou étrangers, des laboratoires publics ou privés.

Interfacial Step Alignment as a Mechanism of Hetero-Epitaxy/Orientation Relationships: The Case of Ag equilibrated on Ni substrates. Part 1 Computer Simulations

Paul Wynblatt\* and Dominique Chatain\*\*

\*Department of Materials Science and Engineering, Carnegie Mellon University, Pittsburgh, PA  
15213, USA

email: pw01@andrew.cmu.edu

\*\* Aix-Marseille University, CNRS, CINaM, F-13288 Marseille, France.

email: chatain@cinam.univ-mrs.fr

**Abstract**

Molecular dynamics simulations of Ag films equilibrated on Ni have been performed for 12 different Ni substrate orientations. The results show that well-equilibrated films display several different orientation relationships (ORs) depending on the Ni substrate orientation: cube-on-cube, twin, oct-cube, and a series of special ORs that are a consequence of the oct-cube OR that develops on Ni(100). It is found that an important feature displayed by the observed ORs is the alignment of the step edges of the Ag film with those of the Ni substrate at the interface. Such alignment is initiated during film formation, but also tends to produce minimum energy interfaces between film and substrate. This feature of hetero-epitaxy and of the resulting ORs has not previously been emphasized.

Key Words: Molecular dynamics simulations, Orientation relationships, Hetero-epitaxy, Mechanism, Interfaces

## 1. INTRODUCTION

The orientation relationship (OR) that develops between an equilibrated film and its underlying substrate is not generally predictable. This is still true, in spite of the large research effort that has been expended on the subject because of its importance in a wide range of technological applications. Even when efforts have been made to equilibrate the deposit on the substrate, so as to eliminate effects due to deposition kinetics, the resulting ORs can be difficult to anticipate.

Much of the research performed to date on hetero-epitaxy and the related ORs of a film on a substrate has focused on relatively simple, low index crystallographic substrate orientations, so that the available information on ORs has been rather limited. Recent experimental advances, such as electron back-scatter diffraction (EBSD) in a scanning electron microscope, have made it possible to probe the ORs displayed by a film of a given material A on a particular polycrystalline substrate B, thereby allowing a large range of ORs to be studied on a given combination of a film/substrate system, under identical experimental conditions (see for example ref [1]). The work described in the companion paper [2], reports on the ORs that are observed by EBSD when a face centered cubic (FCC) film of a metal A is equilibrated on  $\sim 200$  crystallographically different surfaces of the polycrystalline substrate of another FCC metal B. In this paper, we describe the results of modeling the ORs that develop between the same film and substrate materials for 12 different substrate orientations by molecular dynamics simulations. As will be shown, the combination of experiments and modeling provide important insights into the mechanisms by which the observed ORs develop.

In order to understand the factors which govern hetero-epitaxy, and the OR of a thin film of A on a B substrate, many different A-B systems of different structure and lattice parameter have been studied over several decades, from both experimental and a theoretical points of view. These studies have aimed to understand how the lattice mismatch between film and substrate can be accommodated so as to minimize the elastic strain energy in the abutting phases at the interface. One may classify the studies by substrate topography: either the substrate surface is a flat (i.e. step-less) low index terrace, or the substrate surface also contains steps.

On flat surfaces of B, films of A may be coherent, where the lattices of A and B are strained so as to eliminate the mismatch, or they may be semi-coherent and contain misfit dislocations which minimize strain by accommodating much of the lattice mismatch between the film and the substrate. However such dislocation networks may produce a rotation of the film from the nominal orientation relationship on the substrate. The strain due to the interfacial misfit

at interfaces on certain A-B systems can also be fully relaxed by tilting the film and introducing steps at the interface with a frequency that tends to eliminate lattice mismatch [3, 4]. When steps are present at the interface between a misfitting film/substrate system, additional defects known as disconnections may be needed to accommodate the mismatch [5, 6]. In many cases, these interfacial defects cannot fully compensate the discrepancies due to the mismatch [4]. A significant amount of theoretical work has been undertaken to describe the matching of the interfacial disconnections due to steps of different size and/or shape that are present on both sides of the interface. Recent extended analyses [4, 7] show that tilts and rotations of the planes abutting the interface are partitioned between the substrate and the film so as to relax the strains related to the disconnections. All of these analyses are based on a precise description of the arrangements of the atoms of both phases at the interface and rely mostly on experimental studies performed on vicinal substrate orientations [see for example 8].

This paper and its companion [2] have investigated the ORs that develop in Ag films equilibrated on Ni substrates for a large number of substrate surface orientations. The Ag on Ni system was chosen for study for several reasons. 1. It is a relatively simple system since it consists of two metals with the same face centered cubic (FCC) crystal structure, so that many of the variables that could complicate the resulting ORs are absent. 2. Although effects due to lattice mismatch are expected to be present, as the lattice constants are significantly different ( $a_{\text{Ni}} = 0.352\text{nm}$  and  $a_{\text{Ag}} = 0.409\text{nm}$ , respectively), the fact that the ratio  $a_{\text{Ag}}:a_{\text{Ni}} = 1.162$  differs by less than  $\sim 0.4\%$  from the integral ratio of 7:6, implies a likely accommodation of the mismatch by relatively simple interfacial defects. 3. The mutual solubilities of Ag and Ni in the solid state are negligible, so that each of these components of the film-substrate system will remain essentially pure. 4. This system has been the subject of many previous modeling and experimental studies [9-24]; however, both of these types of studies have been limited thus far to simple, low Miller index, substrate orientations.

In previous modeling studies, it has been found that Ag deposited on a Ni{111} substrate grows with a {111} plane parallel to the substrate [23, 24]. It has also been found that Ag grows with its {111} plane parallel to a Ni{100} substrate [13]. These two observations tend to summarize the conventional view that FCC metals will tend to grow either with their {111} surfaces parallel to almost any substrate, or if deposited on a FCC substrate, then a cube-on-cube OR will tend to develop. As we shall see, even in a relatively simple FCC/FCC system such as Ag on Ni, this conventional wisdom does not generally apply when Ag is equilibrated on a variety of different substrate orientations.

The complexity and the wide range of ORs identified in the present studies preclude any systematic analysis of the results using the models mentioned above which invoke detailed combinations of interfacial defects to describe particular ORs. However, our observations will show that an important feature of the ORs adopted by Ag on all the Ni orientations which have been simulated in this paper and measured in the companion paper [2] is the alignment of the interfacial step edges of the Ag and Ni surfaces abutting the interface.

## 2. COMPUTATIONAL APPROACH

### 2.1. Molecular dynamics and lattice statics

Modeling was conducted by molecular dynamics (MD) and lattice statics (LS) simulations, employing the LAMMPS code [25, 26], in conjunction with embedded atom method (EAM) potentials [27]. These potentials include many body effects, and have been used extensively in previous modeling studies of the Ni-Ag system [9-13, 17-20].

Ni substrates of 12 different orientations were studied; these are displayed in the standard stereographic triangle (SST) of Fig. 1. Note that we have made use throughout this paper of a SST with corners located at (100), (110) and (111) orientations. With this choice, all (hkl) within the SST obey the rule  $h \geq k \geq l$ .

Because of the different substrate orientations, slightly different computational cells had to be used. However, the dimensions of the Ni substrates were all approximately 10 nm in the x- and y-dimensions and 2 nm in the z-dimension, and consisted of  $\sim 19,000$  atoms. Periodic boundary conditions were applied in the x- and y-dimensions, but the computation cells were terminated by free surfaces in the z-dimension.

For each Ni orientation, at least two thicknesses of Ag were deposited onto the upper Ni surface:  $\sim 1000$ , and  $\sim 4000$  atoms, corresponding roughly to an adsorbed layer and a structure approaching bulk Ag, respectively. These two configurations will be referred to in what follows as "thin" and "thick" Ag deposits or films. The method used to deposit the Ag onto the Ni substrate will be described below. MD simulations were performed on arrays consisting of Ni and Ag; the arrays were gradually heated from 100 K to 900 K over a period of 200 psec, held at 900 K for periods of up to 12 nsec, in order to approach equilibrium, and then relaxed by LS to remove thermal noise. In most cases, it was found that the structure ceased to evolve significantly after equilibration times of  $\sim 4$  nsec. The temperature of 900 K was selected in order to be close to the equilibration temperature of 923 K used in the experiments of the companion paper [2]. It was also chosen so as to achieve fairly high mobility of Ag for film equilibration in

reasonable simulation times, yet maintain a relatively low mobility of Ni so as to preserve a well-defined substrate orientation. Nevertheless, some minor rearrangements of Ni did occur in the vicinity of the interface.

In some of the previous simulation studies on the nucleation and growth of monolayer deposits on substrates, a great deal of effort has been expended on controlling the energy of the deposited atoms as they arrive at the substrate surface, and nucleation has been studied by adding one deposit atom at a time. Such an approach would have been very time consuming in the present study, where the primary focus was on the orientation relationships that develop between deposit and substrate for films approaching equilibrium bulk-like behavior.

In the case of thin ( $\sim 1000$ -atom) Ag films, the deposits were produced by placing several randomly distributed Ag octahedra, each with one apex just above the Ni substrate, at locations that were approximately one nearest neighbor distance from any surface Ni-atom. Each octahedron consisted of a 44-atom Ag crystallite with its (100) axis perpendicular to the substrate, as shown in Figs 2a and 2b. Thus, except for Ni(100), the orientation of octahedra did not correspond to the orientation of the substrate, thereby avoiding any bias in the eventual near-equilibrium OR. As we shall see later, Ag adopts a (111) interface plane on the Ni(100) substrate; thus even in that case, the OR is not biased by the initial Ag crystallite orientation. In the early stages of simulation, each octahedron slowly collapsed and spread over the substrate to form an adsorbed Ag layer, as shown in Fig. 2c.

In the case of thicker ( $\sim 4000$ -atom) Ag films,  $\sim 3000$  Ag atoms were added to the  $\sim 1000$ -atom equilibrated structures in the form of Ag layers with atoms distributed at random, again ensuring that none of the added atoms were placed any closer than a nearest neighbor distance from either Ni or other Ag atoms. During subsequent MD simulation at 900 K, the random arrangement of Ag atoms crystallized and diminished in thickness. Ag films were considered to be reasonably equilibrated when no further changes in the pole figures, obtained as described in the following section, could be detected by additional MD annealing.

## 2.2. Computation of orientation relationships

While it is possible, in principle, to use the atomic positions of the atoms in a Ag film to generate a simulated diffraction pattern, which then needs to be indexed and interpreted so as to extract an orientation, another simpler and more useful method was used here.

Consider an FCC crystal constructed in a coordinate system where the z-axis is perpendicular to the (hkl) orientation of the surface (x-y plane). The 12 neighbors of any atom lie

along  $\langle 110 \rangle$  directions of the FCC lattice, when referred to the cube axes. Thus, the vectors that correspond to the nearest neighbor directions in the xyz (sample coordinate) system, will yield a  $\langle 110 \rangle$  pole figure (PF) when projected onto a stereogram. The orientation of Ag and Ni in a simulation can thus readily be deduced by computing the average directions of the nearest neighbors of each atom, and displaying them in a stereographic projection. This approach also provides a means of determining whether a Ag film contains crystals of more than a single orientation. An example of the results obtained for the orientation of a thick Ag film on a Ni(511) substrate is given in Fig. 3. The approach described here gives reliable results when there is no significant overlap between the clusters of points that make up the various  $\langle 110 \rangle$  poles. However, when excessive overlap occurs (e.g. Fig. 4 for Ni (110)), then the exact orientation of the regions from which the poles originate becomes less precise.

This approach was implemented by only considering Ag atoms that possess 12 Ag neighbors within a sphere of radius that extends half-way between the first and second neighbor distances. By requiring an atom to have 12 close Ag neighbors, one eliminates consideration of atoms lying at the free surface of the Ag film, as well as those at the Ag/Ni interface. This is useful, as those locations are likely to be associated with relatively large distortions due to atomic relaxation effects and/or the presence of interfacial defects. Thus, the procedure focuses on regions that have a relatively well-ordered Ag bulk-like structure.

### 3. RESULTS

The results obtained from the simulations are displayed in the panels of Fig. 4 in the form of  $\langle 110 \rangle$  PFs, with each panel labeled by the appropriate Ni substrate orientation. The ORs obtained in each case are summarized in Table 1.

#### 3.1. ORs of Ag on the Ni(111) substrate

Our simulations show that Ag is oriented with its (111) plane parallel to the substrate with in-plane close packed  $\langle 110 \rangle$  directions of Ag and Ni displaying twist angles ranging from  $\sim 2^\circ$  to  $4^\circ$  (see Fig. 5a). This occurs in both thin and thick films, when Ag is equilibrated on a perfectly planar substrate. However, when Ag is equilibrated on a Ni(111) substrate with two pre-existing monoatomic steps running along  $\langle 110 \rangle$  directions, it develops a structure with its  $\langle 110 \rangle$  directions aligned with the Ni close packed directions (see Fig. 5b). As shown in Fig. 5b, the steps were located at approximately at  $\frac{1}{4}$  and  $\frac{3}{4}$  of the x-dimension of the computational cell. Figures 5a and b show moiré patterns that reflect the interfacial (misfit) dislocation structure that

develops at the Ag/Ni interface in order to accommodate lattice mismatch. It is interesting to note that the interfacial structure shown in Fig. 5b, for the aligned case, is essentially identical to one obtained several years ago for the Ag/Ni interface by LS simulations [10]. In both structures shown in Figs. 5a and b, the interface planes are oriented such that  $\text{Ag}\{111\} // \text{Ni}(111)$ . The  $\langle 110 \rangle$  PF for the case of the Ag film on the stepped Ni(111) substrate is displayed in Fig. 4. It shows the presence of Ag grains with a cube-on-cube OR on Ni (indicated by the coincidence of Ag poles with each of the Ni poles) as well as twin-oriented Ag grains in the film (indicated by a second set of three Ag poles near the center of the PF, rotated by  $60^\circ$  with respect to the cube-on-cube oriented poles). About 60% of the Ag atoms contribute to the cube-on-cube OR and 40% to the twin OR. In the case of the PF shown in Fig. 4 for Ni(111), the two triangular sets of Ag poles are centered around a  $\langle 111 \rangle$  Ni pole (not shown) which must necessarily lie in the center of the pole figure. For both the Ag cube-on-cube and twin ORs, the in-plane  $\langle 110 \rangle$  directions are parallel to  $\langle 110 \rangle$  poles of Ni.

For other substrate orientations in Fig. 4, described later, the six  $\langle 110 \rangle$  Ag poles that indicate the presence of both cube-on-cube and twin ORs may not seem to be symmetrically disposed about a  $\langle 111 \rangle$  pole (i.e. at the apices of a perfect hexagon). This apparent lack of symmetry occurs because of the distortion imposed by the grid-lines of the pole figure (as illustrated in Fig. 3). It is worth mentioning here that other cases will be encountered where we shall refer to the presence of twin-oriented grains in the Ag film. These are twins with respect to other Ag grains in the film, and do not necessarily lie in twin relation to the Ni substrate. In the present case of a stepped Ni(111) substrate, we observe both cube-on-cube oriented Ag grains as well as their twins. Thus, in this particular case, the Ag grains that are in twin relation to cube-on-cube Ag grains, are also in twin relation to the Ni substrate.

### 3.2. ORs of Ag on the Ni(100) substrate

The structure of Ag on the Ni(100) substrate has also been previously studied. The results of those studies will be discussed in detail in Section 4. In the present simulations, we find that Ag is oriented with a  $\{111\}$  plane parallel to the Ni(100) substrate, in agreement with previous simulations and experimental studies [12, 13, 16, 24]. This OR has been referred to as an "oct-cube" orientation relationship [12, 13]. The  $\langle 110 \rangle$  PF for the Ni(100) substrate orientation shown in Fig. 4 also indicates the presence of at least one type of Ag twin. In addition, this figure shows that the in-plane  $\langle 110 \rangle$  poles of Ag, that lie on the outer circle of the pole figure, are superimposed on the in-plane  $\langle 110 \rangle$  poles of Ni.

### 3.3. ORs of Ag on the Ni(110) substrate

The  $\langle 110 \rangle$  PF for Ag on the Ni(110) substrate orientation is presented in Fig. 4. The  $\langle 110 \rangle$  Ag poles in this figure are considerably more scattered than they were in Fig. 3, and there is significant overlap of the clusters of points representing different Ag  $\langle 110 \rangle$  poles. As a result, it is difficult to isolate the individual poles of Ag, and their identification is therefore only an estimate. In order to fit all possible features of that  $\langle 110 \rangle$  PF, it was necessary to assume four different Ag orientations. These included two variants of Ag{881} (which are in approximate cube-on-cube OR, but tilted by a few degrees from (110) about an in-plane  $\langle 110 \rangle$  direction), and also two variants of Ag{911}, which are in approximate twin-relation to the {881} variants.

### 3.4. ORs of Ag on the Ni substrate orientations along the (100)-(111) edge of the SST

The substrate orientations, Ni(511), (311) and (322), belong to this edge. Their  $\langle 110 \rangle$  PFs shown in Fig. 4, together with those of Ni(100) and Ni(111), show that a gradual transition occurs from the oct-cube Ag OR on Ni(100) to the Ag cube-on-cube and/or twin OR on Ni(111) by a rotation of the Ag orientations with respect to the Ni substrates about a common in-plane  $\langle 110 \rangle$  axis. This gradual transition in OR will be discussed in more detail in Section 4.

### 3.5. ORs of Ag on the Ni substrate orientations along the (111)-(110) edge of the SST

The substrate orientations along this edge include Ni(332) and (551) shown in the  $\langle 110 \rangle$  PFs of Fig. 4. The corresponding ORs are close to being cube-on-cube, with Ag also adopting orientations that are twin-related to the cube-on-cube OR. The ORs obtained for these substrate orientations also display a common in-plane  $\langle 110 \rangle$  direction.

### 3.6. ORs of Ag on the Ni substrate orientations along the (110)-(100) edge of the SST

Along this edge of the SST, Ag orientations undergo another transition, this time from Ag films on Ni(110) that are close to, but not exactly cube-on-cube (with some twin-related Ag), to the Ni(100) substrate where the Ag film displays the oct-cube OR. This transition is illustrated by the  $\langle 110 \rangle$  PFs for Ni(320), (210) and (510) substrate orientations shown in Fig. 4.

### 3.7. ORs of Ag on the Ni(321) substrate

This is the only orientation studied here that lies within the SST. In this case the Ag film predominantly adopts a twin-related orientation to the substrate, as shown in the  $\langle 110 \rangle$  PFs for the Ni(321) orientation in Fig. 4.

## 4. DISCUSSION

### 4.1 Crystallography of surface steps

It is useful to preface the discussion of the results with a description of surface structure by means of the terrace-ledge-kink (TLK) model of surfaces developed by Stranski [28] almost a century ago. For the case of any (hkl) FCC surface within the SST, the orientations of the terrace, ledge and kink can be identified by the micro-facet decomposition scheme of Van Hove and Somorjai [29]. Indeed, any choice of three micro-facets whose normals are linearly independent vectors can serve the purpose. For convenience, we take the micro-facets orientations to be (111), (100) and  $(11\bar{1})$ .

The terrace orientation for a given (hkl) surface is then given by the micro-facet with the largest relative number of atoms, the ledge orientation is given by the micro-facet with an intermediate relative number of atoms, and the kink orientation is given by the micro-facet with the smallest relative number of atoms. The relative numbers of atoms,  $N$ , of the three micro-facets may be expressed by the ratio [29]:

$$N(111):N(11\bar{1}):N(100) = (k + 1):(k - 1):(h - k) \quad (1)$$

As an example, application of Eq. 1 to a (532) surface is shown schematically in Fig. 6.

From Eq. 1, it can also be seen that the (111) surface will consist only of (111) terraces, and similarly, the (100) surface will consist only of (100) terraces. Surfaces along the (100)-(111) edge of the SST, which have indices of the type (hkk), will consist only of a terrace and a ledge. This absence of kinks also applies to surfaces along the (111)-(110) edge of the SST, which have indices of the type (hhl). All other (hkl) surfaces of the SST will have terraces, ledges and kinks. For these cases the surface steps will be made up of both ledges and kinks.

It is also useful to point out that the crystallographic direction of step edges in the TLK model of surfaces can be obtained from the cross product of the terrace normal (identified by Eq. 1) with the normal to the (hkl) surface of interest.

It is generally accepted that the presence of steps, composed of ledges and kinks at the surface of a crystalline substrate, plays an important role in homo-epitaxial film growth.

~~Although recognition of the importance of surface steps has not been extended to hetero-epitaxial growth~~ As we shall see below, the presence of surface steps on the substrate also plays an important role in the equilibrium ORs that develop between Ag and Ni on all substrate orientations. As indicated above, surface steps on FCC crystals occur naturally on all surfaces except  $\{111\}$  and  $\{100\}$ . These steps produce an alignment of the first few deposited atoms that determine the manner in which the deposit develops, and this alignment has a profound effect on the final OR. An example of Ag alignment along steps in the early stages of film formation is shown in Fig. 2c.

#### 4.2. ORs of Ag on Ni(111)

In previous studies of monolayer Ag deposits on Ni(111) [23, 24], the Ag adopts a hexagonal structure in which its close-packed  $\langle 110 \rangle$  directions lie parallel to the close packed  $\langle 110 \rangle$  directions of the Ni substrate at low temperatures, whereas at higher temperatures (the value of which not all authors agree, see [24] and refs therein) the Ag layer is rotated with respect to the substrate by a twist angle of between 1 and 3°. Although the present simulations also show a small twist angle (between 2° and 4°) when the Ni-substrate is initially planar, this rotation disappears when two steps along in-plane  $\langle 110 \rangle$  directions are intentionally created on the initial Ni substrate (see Fig. 5). Since surface steps are an almost unavoidable feature of substrates used for film growth (because of small deviations from an exact (111) substrate orientation) we expect the results obtained in the presence of surface steps to be more realistic for comparison with experiment.

#### 4.3. ORs of Ag on Ni(100)

It has previously been found, by both rotating sphere experiments as well as by epitaxial growth experiments [12, 16], that Ag frequently adopts ORs in which its  $\{111\}$  planes lie parallel to Ni(100) substrates. This oct-cube OR has also been observed previously in simulations of Ag on Ni(100) [13], and of Au on Ni(100) [30] for which the lattice mismatch is almost identical with that of Ag-on-Ni. The OR observed in the present study – Ag $\{111\}\langle 110 \rangle$ //Ni(100) $\langle 110 \rangle$  – is consistent with this previous work, as well as with our own experiments [2].

#### 4.4. ORs of Ag on Ni substrates with orientations lying along the (100)-(111) edge of the SST

Along this edge of the SST, a gradual transition occurs from the oct-cube OR with  $\text{Ag}\{111\}\langle 110\rangle//\text{Ni}(100)\langle 110\rangle$  to a cube-on-cube and/or a twin-related OR with  $\text{Ag}\{111\}\langle 110\rangle//\text{Ni}(111)\langle 110\rangle$ . The  $\langle 110\rangle$  PFs for the orientations along this edge (Ni (100), (511), (311), (322) and (111)) displayed in Figs. 4 show that the close packed in-plane  $\langle 110\rangle$  directions of the Ag film and the Ni substrate are parallel in all cases. These directions also correspond to the directions of the natural TLK surface steps that exist on the Ni and Ag planes on both sides of the interface.

We have attempted to estimate the change in the interface plane of Ag as the Ni substrate orientation varies along this (100)-(111) edge of the SST by means of a simple correlation described in the Appendix. This analyzes the change in the Ag orientation as a gradual rotation of Ag relative to Ni about the common  $\langle 110\rangle$  axis. The results obtained are given in Table 2. When the normalized (hkl) indices for the Ag interface planes in Table 2 are compared with those of Table 1 for the same Ni substrate orientations, one finds remarkable agreement for Ag films on the Ni(511) and (311) substrate orientations, even though the correlation only takes crystal geometry into account, and ignores consideration of lattice mismatch. For the case of the Ni(322) substrate, the results of the simulations for the orientation of the Ag film are quite scattered, and can only be estimated. In spite of this complexity, the results of the appendix correlation given in Table 2 produce a good fit to one of the four orientations identified in Table 1 (with approximate  $(5\ 5\ \bar{3})$  indices). The reasons for the multiple orientations obtained from simulations for the Ni(322) substrate are not clear, but they do imply degeneracy of the interfacial energies associated with the various observed Ag orientations.

Whereas the correlation of the appendix can only be tested against the results of three of the simulations performed here, the companion paper [2] reports experimental results on Ag orientations which correspond to 15 substrate orientations that fall along the (100)-(111) edge of the SST. Those results are compared with predictions of the appendix correlation in Fig. 6 of the companion paper [2], and also yield excellent agreement, even though the correlation does not consider lattice mismatch. While there is substantial evidence in both papers to indicate that lattice mismatch is important in some aspects of the observed ORs, it appears that the sequence of ORs that represent the transition from oct-cube to cube-on-cube and/or twin ORs may be primarily driven by crystal geometry rather than lattice mismatch.

#### 4.5. ORs of Ag on Ni(110)

There have also been a few previous studies of the ORs that develop between Ag and Ni(110). Maurer and Fischmeister [14] used the rotating crystal method, with initially randomly-oriented Ag crystals equilibrated at 1173 K. They identified ORs of Ag(110)//Ni(110) at twist rotations (between close-packed  $\langle 110 \rangle$  directions) of 0 and 70°. They also found tilt ORs of Ag(111) $\langle 110 \rangle$ //Ni(110) $\langle 110 \rangle$  and Ag(211) $\langle 110 \rangle$ //Ni(110) $\langle 110 \rangle$ . Allameh et al. [19] used a variation of the rotating crystal method, in which they sintered Ag crystals with a given initial twist orientation on a Ni(110) substrate. Their experiments used an equilibration temperature of 623 K. They found four different ORs corresponding to Ag(110)//Ni(110), and twist rotations of 0, 35, 55 and 70° between close-packed directions. They also performed LS calculations in conjunction with EAM potentials, in which they computed the Ag/Ni interfacial energy of several (110) twist orientations [20]. These simulations showed that the dependence of interfacial energy on twist angle displayed small cusps at the preferred values of twist angle observed in their experiments.

The present simulations do not assume any particular OR, and unlike the previous LS work, were conducted at high temperature by MD. The results yield four ORs, two ORs that are close to cube-on-cube and which display Ag{881} interface planes with tilts of  $\pm 5^\circ$  from Ni(110) about the in-plane  $\langle 110 \rangle$  direction, and two other ORs that have Ag{911} planes parallel to the interface (with tilts of  $\sim \pm 39^\circ$ ), which are approximately twin-related to the two other Ag orientations. These ORs do not match the observations of Maurer and Fischmeister [14], who observed tilt ORs of 35 and 55°. Our experiments [2] do not contain an example of the Ni(110) orientation. However, several substrate orientations close to Ni(110) display a cube-on-cube orientation, in good agreement with the present results.

#### 4.6. ORs of Ag on Ni substrates with orientations lying along the (111)-(110) edge of the SST

The results obtained for the Ni(332) and (551) substrates are given in the form of  $\langle 110 \rangle$  PFs in Fig. 4 (see also Table 1). It should be noted that, as in the case of the orientations along the (100)-(111) edge of the SST, the in-plane close-packed  $\langle 110 \rangle$  directions of Ni and Ag are parallel, and that these directions also correspond to the direction of step edges on the Ni and Ag interface planes. Both cube-on-cube (with a small tilt of between 2° to 5° about  $\langle 110 \rangle$ ) as well as twin-related orientations are observed in the Ag films.

#### 4.7. ORs of Ag on Ni substrates with orientations lying along the (110)-(100) edge of the SST

The results obtained for the Ni(320), (210) and (510) orientations are displayed in the form of  $\langle 110 \rangle$  PFs in Fig. 4 (see also Table 1). Along this edge of the SST, the direction of steps is not as simple as in the other orientations discussed above. The Ni(320) surface has steps running along the  $[2\bar{3}1]$  direction, and these are almost parallel to the  $[2\bar{3}1]$  direction in the part of the Ag film that is close to having a cube-on-cube OR, with its  $(16\ 9\ \bar{2})$  plane parallel to the interface. The Ag film also contains an orientation,  $\sim (6\ 17\ 0)$ , that is twin-related to  $(16\ 9\ \bar{2})$ , and this twin contains another  $\langle 321 \rangle$  direction in the plane of the interface that is almost parallel to the in-plane  $[2\bar{3}1]$  step direction of the substrate.

In contrast, the Ag film on Ni(210) is oriented almost perfectly in a cube-on-cube OR, and is the only orientation in the simulations for which no Ag twins have been observed. The step edges that run along the  $[001]$  direction of Ni in this case are therefore also parallel to the  $[001]$  step direction on the Ag side of the interface.

The final orientation studied in this region of orientation space, Ni(510), has a more complex OR, because of its proximity to (100), where the Ag film is oriented with its (111) plane parallel to the substrate. Thus, along this edge of the SST there is another transition from a cube-on-cube OR at Ni(210), to Ag orientations that tend to align their (111) planes with the (100) planes of the substrate. Consequently, in the case of the Ni(510) substrate, we find two Ag orientations that have their  $\{111\}$  planes almost aligned with the (100) planes of Ni (see Table 1), and with their step edges running along  $\langle 431 \rangle$ -type directions that are parallel to the  $\langle 100 \rangle$  step directions of the Ni substrate.

#### 4.8. OR of Ag on a Ni(3 2 1) substrate near the center of the SST

As shown in Fig. 4, the Ag film on Ni(3 2 1) is found to display an orientation  $\sim (7\ 2\ 4)$  that is close to a twin of (3 2 1). The Ni(3 2 1) substrate has steps that run in  $\langle 211 \rangle$  directions, and the  $\sim (7\ 2\ 4)$  Ag twin also has steps that run close to  $\langle 211 \rangle$  directions, and those step directions are found to lie within  $\sim 4^\circ$  of each other at the interface.

#### 4.9. Overall picture of Ag ORs on Ni

The observed ORs are summarized in the SST of Fig. 7. ORs corresponding to Ni substrate orientations in the figure are labeled C (cube-on-cube), T (twin), O (oct-cube) and S (special ORs that are a consequence of the transitions from the oct-cube OR at the Ni(100) corner of the SST to either cube-on-cube or twin ORs). It should be mentioned that the limited

number of orientations studied here by MD simulations do not allow a clear delineation of the orientation space occupied by the various ORs; however, a much more complete determination of the orientation regions occupied by these ORs has been possible in the companion paper [2], where over 200 Ni substrate orientations have been investigated. In the present study, most of the Ag films with a cube-on-cube ORs also contain twins of the cube-on-cube ORs. This is not surprising, in view of the low energy of twin boundaries in FCC crystals such as Ag.

#### 4.10. Interfacial step alignment as a unifying feature of observed ORs

The most striking unifying trend in the observed ORs is the universal close alignment in the plane of the interface of the step edges of the Ag film with the step edges of the Ni substrate. Whereas this trend may appear to be similar to the "lock-in" mechanism of epitaxy invoked by Fecht and Gleiter [31] for metals grown on ionic substrates, it occurs for reasons that are quite different from those of the lock-in concept. In the lock-in concept, the surface of the ionic crystal (taken to be a low index plane) is described as "a set of close packed rows separated by relatively deep valleys". The orientation of the metal plane at the interface is then assumed to be determined by having its closest packed row of atoms "lock-in" to the valleys between the closest packed rows of the ionic substrate. This is essentially a lattice matching argument.

In contrast, the present results show that during the initial stages of film formation, deposited Ag atoms tend to align with the step edges of the Ni substrate, since sites adjacent to steps are energetically favorable because of the higher coordination available there for Ag adatoms. Steps are naturally present on all substrate orientations except (100) and (111). However, even in the case of those naturally un-stepped substrate orientations, the complete absence of steps is highly unlikely to occur in experiments, and when steps are present, the deposited Ag atoms preferentially align with the steps (as pointed out above in connection with the OR of Ag on Ni(111) shown in Fig. 5). One question that must still be addressed is whether the Ag/Ni interfacial energy, which must certainly play a role in the equilibrium OR, is minimized by the ORs that are possible within the constraint of step alignment.

Interfacial energies cannot readily be computed from the MD simulations that have been conducted here to determine the ORs that develop between Ag films and Ni substrates. This is because the configurations that emerge from these simulations display non-planar Ag surfaces and somewhat rough Ag/Ni interfaces; in addition, the Ag films often contain twin boundaries, stacking faults and other defects. Since it is not possible to separate out the energies of those defects, or to account for energy changes associated with non-planar interfaces, it is not possible

to isolate the Ag/Ni interfacial energy from our MD simulations. These features also make it very difficult to describe the resulting ORs by means of the detailed descriptions of the interfaces in terms of disconnections [4-7]. However, it is possible to compute interfacial energies from LS simulations (conducted at 0 K) on atomic arrays that consist of a slab of Ag on top of a slab of Ni with a pre-selected OR, as was done by several previous investigators [9-13, 20]. In particular, Allameh et al. [20] studied Ag(110)/Ni(110) twist boundaries and found that the lowest energy occurred for the  $0^\circ$  twist boundary, i.e. for the case consistent with step alignment. Here we have performed similar simulations for Ag(211)/Ni(211) twist boundaries, for 8 different twist angles between step edges, and have also found that the lowest energy interface occurs for  $0^\circ$  twist, adding further evidence that step alignment produces low energy interfaces. However, there are exceptions to this rule. Gao et al. [12] computed the energy of Ag(100)/Ni(100) twist boundaries and found that the lowest energy interface occurred at a twist of  $26.6^\circ$  ( $634 \text{ mJ/m}^2$ ). In contrast, in a later paper [13] they showed that the energy of the Ag/Ni interface with an OR of Ag(111) $\langle 110 \rangle$ /Ni(100) $\langle 110 \rangle$ , i.e. the oct-cube OR, was lower than any of the (100) twist boundaries ( $437 \text{ mJ/m}^2$ ). This result is consistent with the results of the present simulations, and explains why lower energy interfaces consisting of Ag(111) parallel to Ni(100), with aligned close packed directions, are found in the simulations rather than Ag(100) twist interfaces. Thus, although zero twist may frequently lead to minimum energy interfaces, this may not always be the case.

It is useful to identify the reason for the frequent increase in interfacial energy when steps cross each other at interfaces with a finite twist angle between step edges. The results of our simulations on Ag(211)/Ni(211) twist interfaces indicate that significant distortion occurs where steps intersect. This is illustrated for the Ag(211)/Ni(211)  $39.2^\circ$  twist boundary in Fig. 8. Figure 8a shows the initial configuration of the near-interface atom planes, and Fig. 8b shows the configuration obtained after a LS relaxation of the system. The relaxed configuration shows that the Ni atom rows (i.e. step edges) remain fairly straight, whereas the Ag atom rows are quite perturbed near the points of intersection with the Ni rows. In addition, a clear tendency in these distortions can be seen to favor step alignment. The larger distortion on the Ag side of the interface is a result of the lower elastic modulus of Ag as compared to that of Ni. These large distortions at step intersections are the source of the interfacial energy increase with twist angle, since the number of such intersections, per unit area, increases with increasing twist angle. Furthermore, one possible reason for the lack of a minimum in energy for (100) Ag/Ni interfaces at  $0^\circ$  twist in the computations of Gao et al. [12], is that no steps are present in perfect (i.e. un-

stepped) (100) twist interfaces of their simulations. For such un-stepped interfaces, a high coincidence interface such as the  $26.6^\circ$  twist boundary, may indeed produce the minimum energy interface as a function of twist angle. However, as noted above, even the lowest energy  $26.6^\circ$  twist (100) interface is higher in energy than the step-aligned Ag(111)//Ni(100) interface.

A minimum energy at  $0^\circ$  twist interfaces is, of course, well known from previous work on grain boundaries (GBs). This arises from the development of screw dislocation arrays at the GB that increase in density with increasing twist angle. When the crystallographic planes that delimit the GB are identical, i.e. in symmetrical twist GBs, the GB as well as its energy vanishes at  $0^\circ$  twist. But even in the case of asymmetric GBs delimited by different crystallographic planes, which contain a tilt component, and where the GB does not vanish at  $0^\circ$  twist angle between step directions, computer simulations have shown that  $0^\circ$  twist GBs also display an energy minimum [32]. In addition, this feature has been used previously to develop successful models of GB energy and GB segregation, which invoke the effects of step intersections to account for GB energy change [33, 34].

The above considerations support the view that, whereas step alignment in the present simulations may occur initially because the first deposited atoms tend to diffuse and attach themselves to step edges for energetic reasons, this type of configuration also creates the nuclei for  $0^\circ$  twist interfaces which tend to display minimum energy.

One last point needs to be made. If one considers the  $\langle 110 \rangle$  PFs for all Ni substrate orientations from Ni(100) to Ni(551) in Fig. 4, i.e. all Ni orientations lying along the (100)-(111) and (111)-(110) edges of the SST, there is always an alignment of the  $\langle 110 \rangle$  Ag and Ni poles at the east and west points of the PFs. These poles represent in-plane  $\langle 110 \rangle$  directions, as well as the step edge directions of the respective Ag and Ni abutting surfaces represented in those plots. Indeed,  $\langle 110 \rangle$ -oriented surface steps only occur along the (100)-(111) and (111)-(110) edges of the SST. In the case of the  $\langle 110 \rangle$  PFs for Ni substrate orientations from Ni(320) to Ni(321) of Fig. 4 (i.e. either along the (110)-(100) edge of the SST or for the orientation that lies within the SST) there are no in-plane  $\langle 110 \rangle$  directions, and no  $\langle 110 \rangle$ -oriented steps. Nevertheless, these figures display rather close superposition of  $\langle 110 \rangle$  Ni and Ag poles at locations near the edge of the respective stereograms (i.e. close to but not exactly in-plane). This feature can also be explained by a close alignment of steps on the two sides of the interface, as illustrated in Fig. 9. The figure shows the schematic top view of a step on a high index Ni surface, with Ag atoms attached to the step edge. In general there will be kinks on the step that cause it to deviate from a  $\langle 110 \rangle$  ledge direction. Although the Ag atoms are more or less aligned with the step, this

alignment is imperfect because of atomic size differences due to lattice mismatch. However, the approximate alignment with the step also leads to an approximate alignment with the close packed directions, even though those directions do not lie in the plane of the interface. Thus, all the features observed in the simulations and the corresponding ORs can be reconciled by either an exact or an approximate alignment of steps on both sides of the Ag film/Ni substrate interface.

A test of the importance of interfacial step alignment, as a unifying feature of observed ORs, has been performed on the much larger set of OR data obtained in the companion paper [2]. The good agreement obtained in that case further validates this interpretation of the generation of equilibrium ORs. This feature of equilibrium ORs in hetero-epitaxy has not previously been emphasized; it appears to explain the origin of ORs, and corresponds to ORs that frequently produce minimum interfacial energy.

## 5. CONCLUSIONS

The ORs that develop in Ag films equilibrated on Ni substrates have been investigated here by MD simulations for substrates having a greater range of orientations than previously studied. Several different ORs have been observed: cube-on-cube, twin, oct-cube, and special ORs. These latter are a consequence of the transition from the oct-cube OR, which develops at the Ni(100) corner of the SST to the cube-on-cube and/or twin ORs that develop at the Ni(111) corner of the SST. It is proposed that all of the various observed ORs develop as the result of an alignment of the step edges of the Ag film with those of the Ni substrate at the Ag/Ni interface. Since step intersections at the interface are often associated with an energy penalty, step alignment, which occurs in the early stages of film formation, also tends to lead to minimum energy interfaces between film and substrate. Interfacial step alignment is a concept that has not previously been stressed as a feature of hetero-epitaxy and/or ORs, and one which deserves to be tested in other systems.

Acknowledgments. PW wishes to acknowledge the use of resources of the National Energy Research Scientific Computing Center, which is supported by the Office of Science of the U.S. Department of Energy under Contract No. DE-AC02-05CH11231. DC wishes to thank Prof. G.S. Rohrer for providing support at Carnegie Mellon University during part of a sabbatical leave from CINaM in Marseille. In addition, the authors wish to thank Profs. G.S. Rohrer and A.D. Rollett for useful discussions, and Prof. W.D. Kaplan for his valuable comments on the manuscript prior to submission.

## Appendix

On a Ni(100) substrate, the Ag crystal is oriented with a  $\{111\}$  plane (say the (111) plane) parallel to the substrate, in the oct-cube OR. At the other end of the (100)-(111) edge of the SST, i.e. on the Ni(111) substrate, the Ag crystal is oriented with another  $\{111\}$  plane (say the  $(11\bar{1})$  plane) parallel to the substrate to produce either a cube-on-cube or a twin OR. For an intermediate case along this edge of the SST, let the angle between Ni(hkl) and Ni(100) be  $\theta$ , as shown schematically in Fig. A1. Thus,  $\theta$  will vary from 0 to  $54.7^\circ$  as Ni(hkl) changes from (100) to (111) by rotation about a common  $[01\bar{1}]$  direction that lies at the intersection of (100) and (111). Consider now the Ag side of the interface. Let the angle between Ag(hkl) and Ag(111) be  $\phi$ . Thus,  $\phi$  will vary from 0 to  $70.5^\circ$  as Ag(hkl) changes from (111) to  $(11\bar{1})$  by rotation about a common  $[1\bar{1}0]$  direction that lies at the intersection of (111) and  $(11\bar{1})$ . This will result in Ag(hkl) that lies along the (111) to  $(11\bar{1})$  arc of a stereogram that extends past (110) of the SST into the adjacent stereographic triangle. When referred back to the SST, all Ag orientations will therefore lie on the (111)-(110) edge. If we assume that the changes in both the Ni and Ag orientations are linear in rotation angles, then:

$$\phi = (70.5^\circ/54.7^\circ) \theta = (1+15.8^\circ/54.7^\circ) \theta \quad (\text{A1})$$

where  $15.7^\circ (= 70.5^\circ - 54.7^\circ)$  represents the relative angle of rotation between Ag and Ni. The results of applying this simple correlation are summarized in Table 2.

## References

1. Burbure NV, Salvador PA, Rohrer GS (2010) Orientation and phase relationships between titania films and polycrystalline BaTiO<sub>3</sub> substrates as determined by electron backscatter diffraction mapping, *J Am Ceram Soc* 93:2530-2533.
2. Chatain D, Wynblatt P, Rollett AD, Rohrer GS (2015) Interfacial step alignment as a mechanism of hetero-epitaxy/orientation relationships: The case of Ag on Ni. Part 2 experiments, *J Mater Sci* 50(15), 5276-5285
3. Du R, Flynn CP (1990) Asymmetric coherent tilt boundaries formed by molecular beam epitaxy, *J Phys: Condens Matter* 2:1335-1341.
4. Hirth JP, Pond RC (2010) Strains and rotations in thin deposited films, *Phil Mag* 90:3129–3147.
5. Hirth JP (1994) Dislocations, steps and disconnections at interfaces, *J Phys Chem Solids* 55: 985-989.
6. Hirth JP, Pond RC (1996) Steps, dislocations and disconnections as interface defects relating to structure and phase transformations, *Acta Mater* 44:4749-4163.
7. Hirth JP, Pond RC, Hoagland RG, Liu XY, Wang J (2013) Interface defects, reference spaces and the Frank–Bilby equation, *Progress in Materials Science* 58:749–823.
8. Aindow M, Pond RC (1991) On epitaxial misorientations, *Phil Mag A* 63:667-694.
9. Dregia SA, Bauer CL, Wynblatt P (1986) The structure and composition of interphase boundaries in Ni/Ag-(001) thin films doped with Au, *Mater Res Soc Symp Proc* 56:189-194.
10. Dregia SA, Wynblatt P, Bauer CL (1987) Epitaxy for weakly interacting systems of large misfit, *Mater Res Soc Symp Proc* 94:111-120.
11. Dregia SA, Wynblatt P, Bauer CL (1989) Computer simulations of epitaxial interfaces, *Mater Res Soc Symp Proc* 141:399-404.
12. Gao Y, Dregia SA, Shewmon PG (1989) Energy and structure of (001) twist interphase boundaries in the Ag/Ni system, *Acta Metall* 37:1627-1636.
13. Gao Y, Shewmon PG, Dregia SA (1989) Investigation of low-energy interphase boundaries in Ag/Ni by computer simulation and crystallite rotation, *Acta Metall* 37:3165-3175.
14. Maurer R, Fischmeister HF (1989) Low energy heterophase boundaries in the system silver/nickel and in other weakly bonded systems, *Acta Metall* 37:1177-1189.
15. Gao Y, Merkle KL (1990) Atomic Structure of Ag/Ni interfaces, *Mater Res Soc Symp Proc* 183:39-44.

16. Gao Y, Merkle KL (1990) High-resolution electron microscopy of metal/metal and metal/metal-oxide interfaces in the Ag/Ni and Au/Ni systems, *J Mater Res* 5:1995-2003.
17. Gumbsch P, Daw MS, Foiles SM, Fischmeister HF (1991) Accommodation of the lattice mismatch in a Ag/Ni heterophase boundary, *Phys Rev B* 43:13833.
18. Gumbsch P (1992) Atomistic study of misfit accommodation in cube-on-cube oriented Ag/Ni heterophase boundaries, *Z Metallkd* 83:500-507.
19. Allameh SM, Dregia SA, Shewmon PG (1994) Structure and energy of (110) twist boundaries in the Ag/Ni system, *Acta Metall Mater* 42:3569-3576.
20. Allameh SM, Dregia SA, Shewmon PG (1996) Energy of (110) twist boundaries in Ag/Ni and its variation with induced strain, *Acta Mater* 44:2309-2316.
21. Floro JA, Thompson CV, Carel R, Bristowe PD (1994) Competition between strain and interface energy during epitaxial grain growth in Ag films on Ni(001), *J Mater Res* 9:2411-2424.
22. Gumbsch P. (1997) The accommodation of lattice mismatch in Ag/Ni heterophase boundaries, *J Phase Equilibria* 18:556-561.
23. Mroz S, Jankowski Z, Nowicki M (2000) Growth and isothermal desorption of ultrathin silver layers on the Ni(111) face at the substrate temperature from 180 to 900 K, *Surface Sci* 454:702-706.
24. Chambon C, Creuze J, Coati A, Sauvage-Simkin M, Garreau Y (2009) Tilted and nontilted Ag overlayer on a Ni(111) substrate: structure and energetics, *Phys Rev B* 79:125412, and references therein.
25. Plimpton SJ (1995) Fast parallel algorithms for short-range molecular dynamics, *J Comp Phys* 117:1-19.
26. <http://www.cs.sandia.gov/~sjplimp/lammps.html>
27. Foiles SM, Baskes MI, Daw MS (1986) Embedded-atom-method functions for the fcc metals Cu, Ag, Au, Ni, Pd, Pt, and their alloys, *Phys Rev B* 33:7983.
28. Stranski IN (1928) Zur Theorie der Kristallwachstums, *Z Phys Chem* 136:259-277.
29. van Hove MA, Somorjai GA (1980) A new microfacet notation for high-Miller-index surfaces of cubic materials with terrace, step and kink structures *Surface Sci* 92:489-518.
30. Luedtke WD, Landman U (1991) Metal-on-metal thin-film growth: Au/Ni(001) and Ni/Au(001), *Phys Rev B* 44:5970-5972.
31. Fecht H, Gleiter H (1985) A lock-in model for the atomic structure of interphase boundaries between metals and ionic crystals, *Acta Metall* 33:557.

32. Wolf D (1990) Structure-energy correlation for grain boundaries in f.c.c. metals - IV. Asymmetrical twist (general) boundaries, *Acta Metall Mater* 38:791-798.
33. Wynblatt P, Takashima M (2001) Correlation of grain boundary character with wetting behavior, *Interface Sci* 9:265-273.
34. Wynblatt P, Shi Z (2005) Relation between grain boundary segregation and grain boundary character in FCC alloys, *J Mater Sci* 40:2765-2773.

## Figures

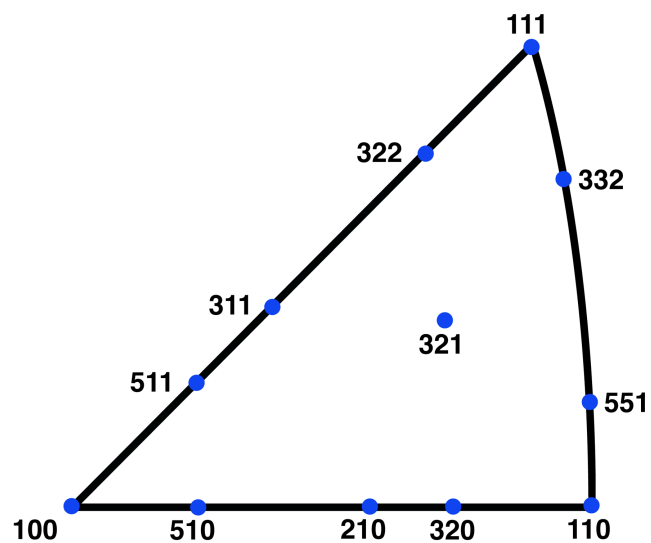


Figure 1. Standard stereographic triangle, showing orientations of the Ni substrates for which simulations were performed.

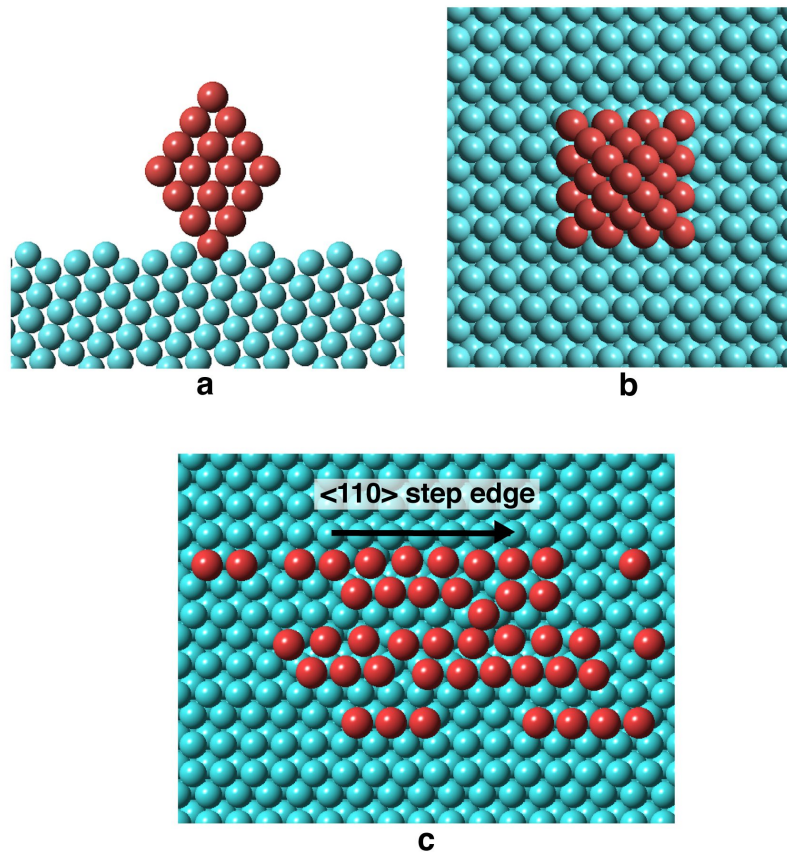


Figure 2. Example showing the method of Ag deposition for thin Ag films using collapsing octahedra. The example uses a Ni(511) substrate. (a) Side view, and (b) top view of octahedron, prior to MD simulation. (c) Top view of octahedron after MD simulation, showing collapse and spreading on the substrate, as a result of gradual heating to 800 K, holding at 800 K for 40 psec, and followed by LS relaxation. Similar simulations at temperatures of 700 K, or below, do not lead to complete spreading of the octahedron. (Ag atoms red, Ni atoms blue: color on line). Part (c) of the figure also illustrates alignment of Ag atoms along the step edges of the Ni(511) substrate that occurs at an early stage of film formation.

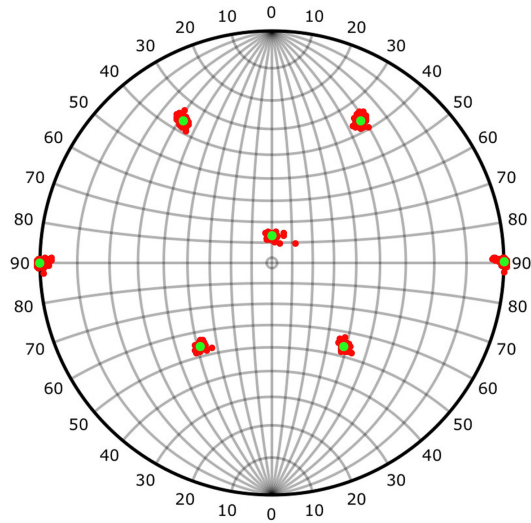
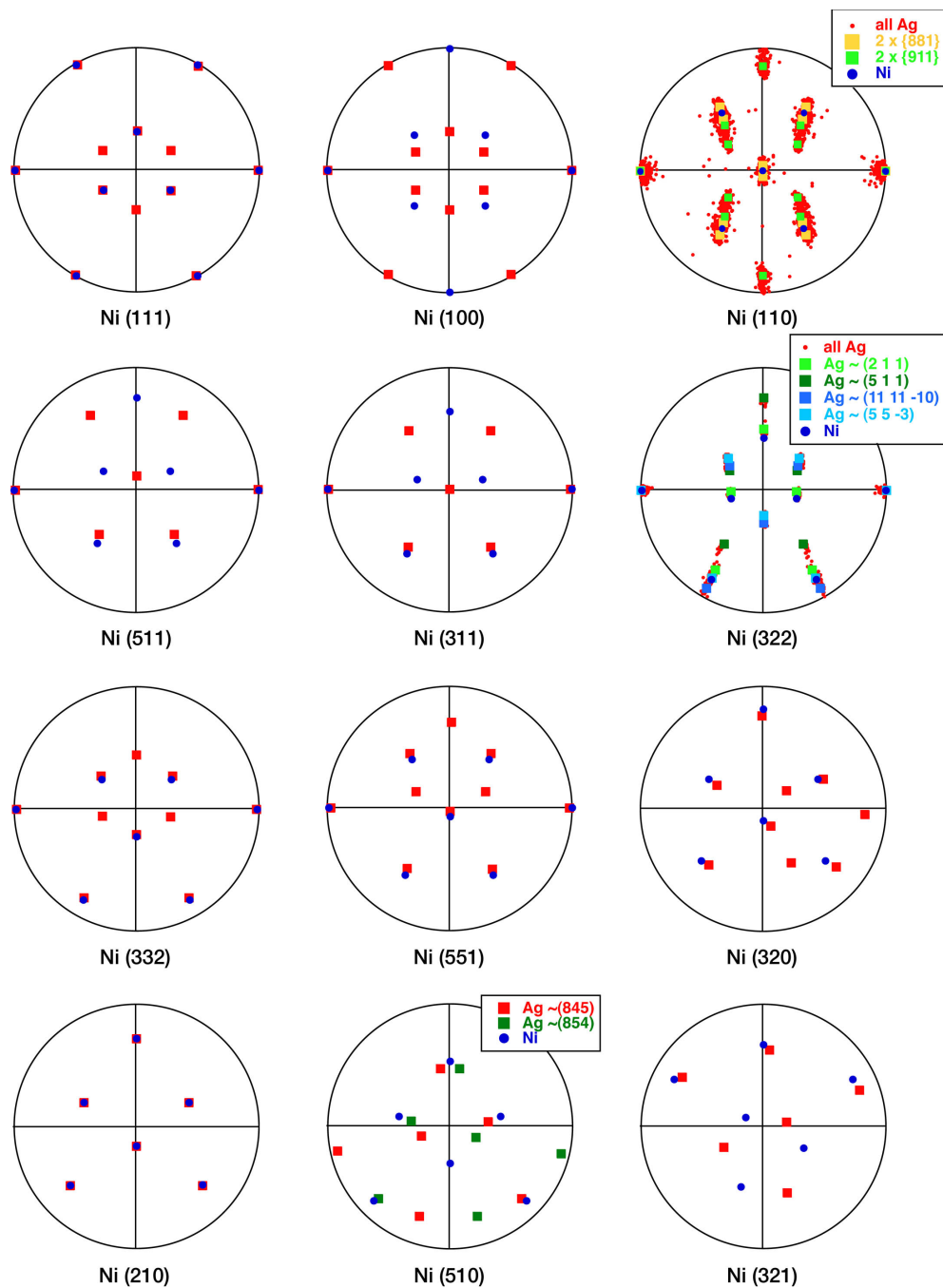


Figure 3. Example to illustrate the method used to determine the orientation of Ag deposit films after MD simulation and relaxation. The figure shows a projection of Ag nearest neighbor vectors onto a stereographic projection for the case of an Ag film equilibrated on Ni(511), to yield a  $\langle 110 \rangle$  pole figure of the Ag deposit. Small red points show the scatter of poles obtained from 500 Ag atoms in the deposit. Large green points represent the average positions of the red points (color on line). The computed Ag film interfacial plane orientation is approximately (331).



**Figure 4.** Each panels displays the "northern hemisphere" of the  $\langle 110 \rangle$  PFs of Ni and Ag for all the substrate orientations studied (averaged Ni poles: round blue symbols, averaged Ag poles: square symbols in red and other colors). The Ni substrate orientation identifies each panel. Note that in the panels for the Ni(110) and (322) substrates, all Ag poles, displayed as small red symbols, show some scatter with significant overlap; estimated average Ag pole locations are indicated by square symbols of various colors.

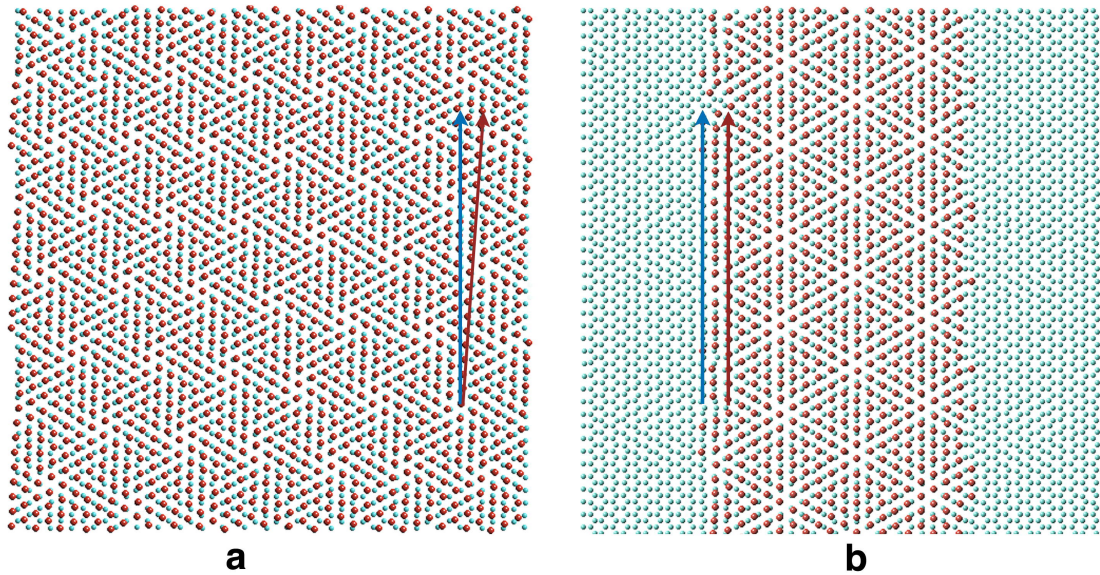


Figure 5. Slices of equilibrated thick Ag films on Ni(111) showing 2 atomic layers from the region near the interface, in which the atom size has been reduced to improve visibility though the slice. (Ag red, Ni blue, arrows indicate  $\langle 110 \rangle$  directions). (a) Ag on a planar Ni substrate showing a twist angle of  $\sim 3.8^\circ$ , and (b) Ag on a stepped Ni substrate, where  $\langle 110 \rangle$  Ag steps are aligned with the  $\langle 110 \rangle$  Ni steps resulting in a zero twist angle.

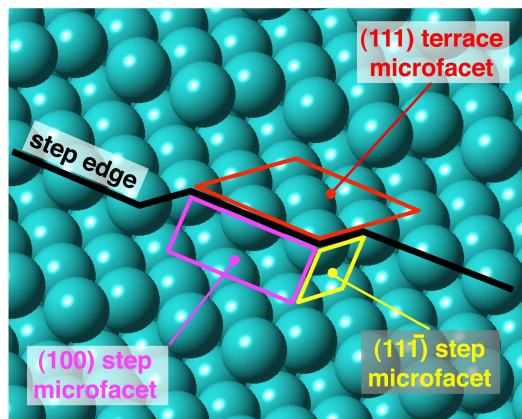


Figure 6. Schematic of van Hove and Somorjai micro-facet decomposition scheme [29] as applied to a FCC (532) TLK surface.

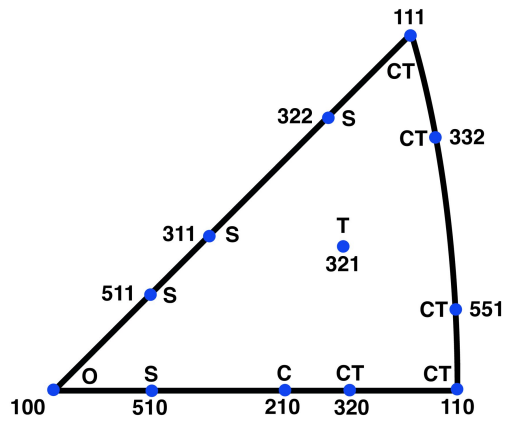


Figure 7. SST summarizing the ORs observed in simulations. ORs in the figure are labeled C (cube-on-cube), T (twin), O (oct-cube) and S (special) ORs that reflect the gradual transition from the oct-cube OR on Ni(100) to either twin or cube-on-cube ORs.

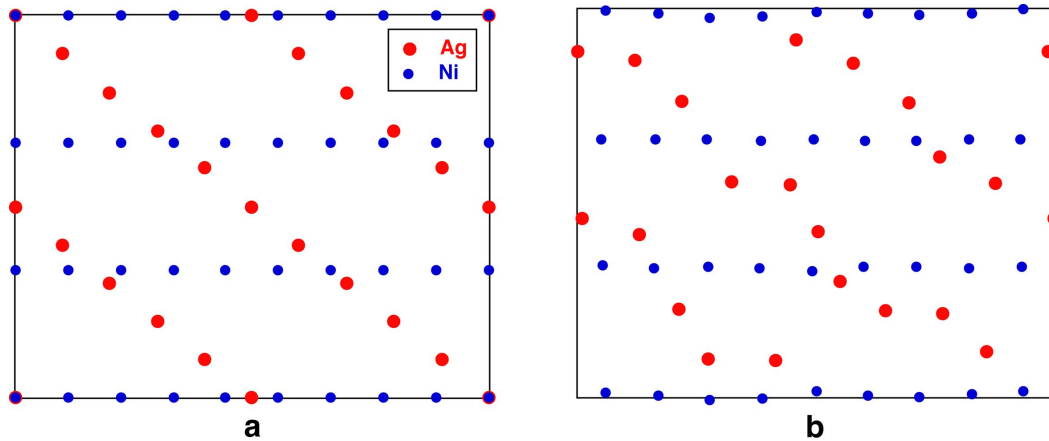


Figure 8. Interface structure of Ag(211)/Ni(211) for a twist angle of  $39.2^\circ$  showing the Ag atoms in red and the Ni atoms in blue; (a) prior to LS relaxation the Ag atoms are aligned along  $\langle 110 \rangle$  step edges, (b) after relaxation the Ag atoms close to the intersections with the  $\langle 110 \rangle$  step edges of Ni tend to align themselves parallel to these edges.

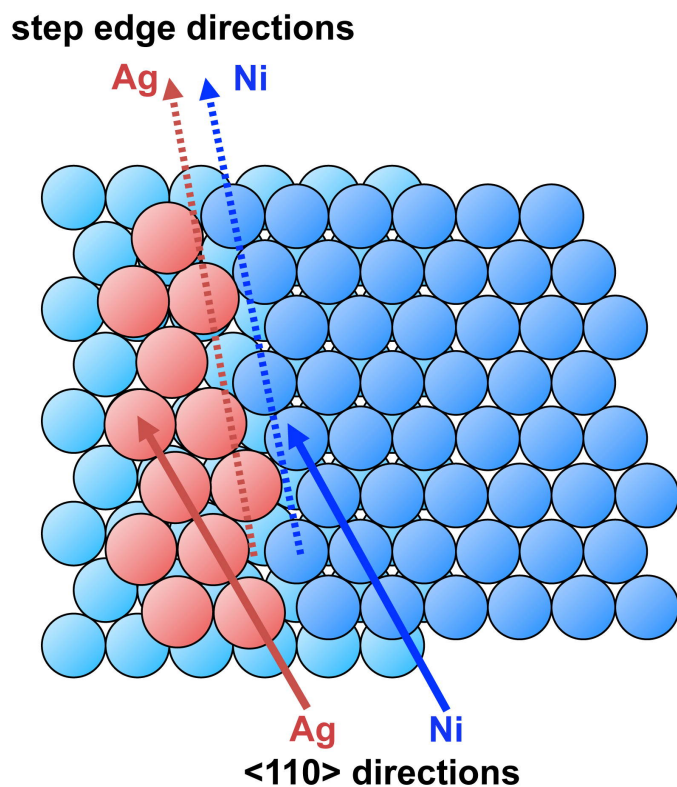


Figure 9. Schematic top view of a step on high-index Ni surface (Ni atoms blue) with Ag atoms (red) attached to the step edge. The arrows indicate step directions and close packed directions in both the Ni substrate and the Ag atoms attached to the step.

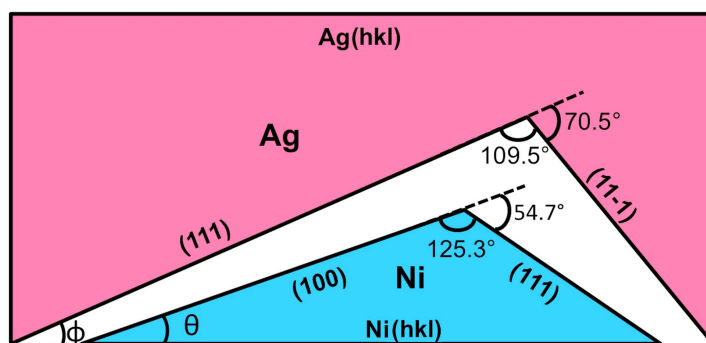


Figure A1. (Appendix figure) Schematic of orientation relationship of Ag on Ni along the (100)-(111) edge of the SST.